MULTICOMPONENT ANALYSIS OF FTIR SPECTRA: QUANTIFICATION OF AMORPHOUS AND CRYSTALLIZED MINERAL PHASES IN SYNTHETIC AND NATURAL SEDIMENTS

JACQUES BERTAUX[1], FRANÇOIS FRÖHLICH[2], AND PHILIPPE ILDEFONSE[3]

[1] *ORSTOM, Laboratoire des Formations Superficielles, Programme PVC, Département RED, 72, route d'Aulnay, 93143 Bondy cedex, France*

[2] *Laboratoire de Géologie du Muséum National d'Histoire Naturelle, 43, rue Buffon, 75005 Paris, France*

[3] *Laboratoire de Minéralogie–Cristallographie, UA CNRS 09, Universités Paris 6 et 7 and IPGP, 4 place Jussieu, 75252 Paris cedex 05*

ABSTRACT: **The study of weathering and erosion processes requires the establishment of a mass balance of minerals from the soils towards the sedimentation area. This calls for the development of quantitative tools that can be applied to mixtures of finely divided and sometimes poorly crystallized minerals found in soils and sediments. We present here the use of Fourier transform infrared (FTIR) absorbance spectroscopy in the mid-infrared as a method to calculate mineral modes for such materials.**

Samples were prepared using the KBr disc method. This ensures that Lambert–Beer's law is valid. A quantitative determination of the mineral content from various blends was performed by making a multicomponent analysis of the experimental spectrum using the spectra of each component in the mixture. To check the validity of the procedure, the multicomponent analysis was performed on spectra from synthetic mixtures of standard minerals (quartz, kaolinite, gibbsite, amorphous silica). Good agreement between actual and computed wt % was obtained in the range 1315–315 cm^{-1}.

This application of FTIR spectroscopy was used to quantify the mineral components of a lacustrine sediment cored at Salitre, Minas Gerais, Brazil. The major phases are organic matter, kaolinite, gibbsite, quartz, anatase, and amorphous silica (phytoliths and sponge spicules). Fifty-three samples were analyzed. Quantitative results from FTIR spectroscopy were compared to chemical analyses to assess the validity of the method for the natural sediments. Phases with no sharp diagnostic spectral features, such as anatase or amorphous silica, were quantified using the multicomponent analysis.

The variations of the main mineral phases along the core reflect the mechanisms of transfer from the surrounding soils to the sediment area and the role of the vegetal cover over the drainage area.

INTRODUCTION

The major components of lacustrine sediments carry environmental information of various form. They are an integration of components from two distinct environments (Dean 1993): (1) the external terrestrial environment of the drainage basin and beyond (allochthonous components, mainly from soils), and (2) the internal lake environment (autochthonous components). The allochthonous components are tracers of weathering and erosion processes. Their behavior during their transport from soils to the lake results from several factors, including the type of soils, the vegetation cover, the climate, and the drainage pattern over the drainage basin. The autochthonous components are indicators of processes acting within the lake and within the postdepositional (diagenetic) environment. In order to assess environmental conditions prevailing during sedimentation it is useful to perform mass-balance calculations among these various sources. However, quantitative determination of major mineral phases in soils or sediments remains a difficult task, because the complexity of these natural mixtures leads to the difficulty of using conventional methods such as X-ray diffraction or optical microscopy. The methodology presented in this paper was developed to study tropical lacustrine sediments which contain common detrital minerals such as quartz, kaolinite, gibbsite, and amorphous mineral compounds such as biogenic silica in the form of phytoliths, diatoms, and sponge spicules; these mineral phases are associated with organic matter, either transported to the sedimentary basin or produced in situ. The relative proportions of these constituents can vary to form mixtures ranging in composition from slightly organic sediments to almost pure organic deposits like peats. Observation of these variations with time helps in describing the climate variability during the late Quaternary. Such a compositional variability is also found in marine sediments, in soils that represent the main source of materials available for erosion and sedimentation, and in eolian dusts (Drees et al. 1993; Rognon et al. 1996).

Various techniques have been proposed to monitor the compositional changes of soils or sediments. Elemental chemical analysis yields very accurate results, but a given element may be present in more than one phase and the mineral composition cannot be deduced from the elemental composition. Data from selective chemical dissolution, usually used by soil scientists (Jones 1969; Teissier et al. 1979), are difficult to interpret in the case of complex mixtures in which several readily soluble phases are present (Gehlen and Van Raaphorst 1993). X-ray diffraction, although used largely for semiquantitative and quantitative determination in rocks and sediments, suffers from strong limitations due to the difficulty of analyzing amorphous compounds and disordered clay minerals. Moreover, organic matter can lead to great difficulties when preparing samples for X-ray diffraction. For example, attempts to eliminate it with strong oxidizers can promote the formation of new compounds. Petrographic techniques such as the optical microscope are useful for a qualitative description of the samples, but their use for quantifying finely divided materials is impossible.

The aim of this paper is to investigate the use of Fourier transform infrared (FTIR) transmittance/absorbance spectroscopy, in the mid-infrared region, for determining the relative abundances of the mineral components in sediments. First, the proposed technique was tested on synthetic mixtures of crystallized and amorphous mineral components. Then, natural sediments, originating from Salitre, west Minas Gerais state (Brazil), were analyzed by FTIR spectroscopy, and the resulting modal analyses were compared to chemical determinations of major elements on the same samples. The abundances of major mineral phases in the sediment are discussed in light of environmental changes over the drainage basin as revealed by the pollen analysis.

MATERIALS AND METHODS

Materials

Reference Compounds.—The reference compounds consist of: natural quartz; amorphous silica, or opal A according to the nomenclature of Jones and Segnit (1971), constituted with Hexactinellid sponge spicules of Holocene age, collected in the central Indian Basin (Fröhlich 1989); kaolinite from Macon, Georgia (USA), supplied by Wards; and synthetic gibbsite supplied by Aluminium Pechiney. Purity of all samples was checked by X-ray diffraction.

Synthetic Mixtures.—Synthetic mixtures of these reference compounds (Tables 1, 2) were prepared by weighing.They consist either of binary mixtures (quartz–kaolinite, quartz–gibbsite), or four-component mixtures (quartz, kaolinite, gibbsite, amorphous silica). These mineral components were chosen because they are very widespread in soils and sediments.

Soils and Sediments.—The Salitre ultramafic-alkaline complex (west of Minas Gerais State, Brazil) has a central, dolina-shaped depression partially

JOURNAL OF SEDIMENTARY RESEARCH, VOL. 68, NO. 3, MAY, 1998, P. 440–447
 1073-130X/98/068-0440/$03.00

TABLE 1.—*Results of the quantitative analyses of two components synthetic mixtures.*

Synthetic Mixture	Quartz Actual wt %	Quartz Computed wt %	Kaol. Actual wt %	Kaol. Computed wt %	Gibb. Actual wt %	Gibb. Computed wt %
q80-k20	80	73.3	20	20.7		
q60-k40	60	58.8	40	36.0		
q40-k60	40	38.2	60	57.8		
q20-k80	20	19.6	80	75.9		
q80-g20	80	77.7			20	18.9
q60-g40	60	56.4			40	38.8
q40-g60	40	40.3			60	60.3
q20-g80	20	19.1			80	81.3

Kaol. = Kaolinite; Gibb. = Gibbsite.

TABLE 2.—*Results of the quantitative analyses of synthetic mixtures with four components.*

Synthetic Mixtures		Quartz wt %	Kaolinite wt %	Gibbsite wt %	Amorphous Silica wt %
M1	1	25	50	20	5
	2	25.1	49.4	21.1	5.1
M2	1	20	50	20	10
	2	21.0	48.6	20.4	9.2
M3	1	10	60	15	15
	2	13.1	57.8	17.8	14.9
M4	1	15	40	25	20
	2	19.5	42.0	25.5	21.0
	3	39.2	43.2	24.0	n.d.

1 = actual wt %; 2 = computed wt %; 3 = computed wt % after multicomponent analysis using only three end-members spectra (quartz + kaolinite + gibbsite); n.d. = not determined.

filled by sediments. A thick, loose latosolic cover (goethite, gibbsite, kaolinite, quartz, anatase, crandallite-family phosphates) surrounds the depression (Sondag et al. 1996). Fifty-three samples were collected from a 6 m-long core (LC3) retrieved from the lake. A high organic-matter content (especially plant fibers) characterizes most of the core, as indicated by high loss on ignition and total organic carbon contents (ranging from 10 to 50%). X-ray diffraction and optical microscopy data showed that quartz, kaolinite, gibbsite, anatase, and amorphous silica are the main inorganic components of the Salitre sediments (Sondag et al. 1993). Because reference spectra are required for quantitative analysis of the natural sediments by our method (see below), the following mineral and organic phases were used for this purpose:

–quartz, gibbsite, and amorphous silica already used in the synthetic mixture;

–a kaolinite separated from a soil near Manaus (Brazil); it was chosen because of its spectral resemblance to the kaolinite from the Salitre sediment; both are poorly ordered, as demonstrated by the relative amplitude of the structural OH bands between 3600 and 3700 cm^{-1} (Cases et al. 1982), with three broad bands at 3620, 3650, and 3698 cm^{-1}. Kaolinite was separated from the bulk sample after suspension in deionized water and centrifugation (10 min at 3000 rpm);

–an anatase reference sample, hand-picked from a soil around the Salitre sedimentary deposit;

–two different references were used for organic matter. For the bottom part (160–600 cm), the sediment between 160 and 260 cm is purely organic (peat), and the spectrum of a sample at 164 cm was used as the reference spectrum for organic matter. In the upper part (0–160 cm), the sediment between 0 and 70 cm is composed of organic matter mixed with amorphous silica (phytoliths and sponge spicules). A reference spectrum for organic matter was obtained by mathematically subtracting the amorphous silica component from the spectrum of a sample in this part of the core.

Methods

Background of UVVIR Quantitative Analysis.—Spectroscopy in the ultraviolet (UV, 0.2–0.4 μm), visible (V, 0.4–0.7 μm), near-infrared (NIR, 0.7–5 μm), and mid-infrared (MIR, 2.5–40 μm) regions has been used extensively for mineralogical studies. The UVVNIR region (0.2–5 μm) is favorable to assess the mineralogy of a mixture because various mechanisms can produce photon absorption (Gaffey et al. 1993): electronic transitions in molecular orbitals, vibrational transitions in molecules and crystals, and electronic transition within and between atoms. On the other hand, MIR is the region where the major rock-forming minerals have their fundamental molecular vibration bands (Farmer 1974; Salisbury 1993). Spectroscopic data are measured either in transmission or in reflection mode, and spectra record absorption or emission features. Reflectance spectroscopy has been much investigated as a method for mineralogical analyses of planetary surfaces via remote sensing (Bishop et al. 1996), and as a method for quantitative analysis of mineral mixture (Mustard and Pieters 1989; Sunshine and Pieters 1993). Determination of hematite and goethite concentrations in geological materials was performed by visible reflectance spectroscopy (Deaton and Balsam 1991; Barranco et al. 1989). Balsam and Deaton (1996) used UVVNIR reflectance spectroscopy to estimate organic carbon, opal, and carbonate in marine sediments. Bishop et al. (1996) demonstrated a correlation between band depths of organic and carbonate features measured on IR reflectance spectra of lacustrine sediments from Antarctica and weight percent carbon (as carbonate or as organic) of the same sediments.

Outline of IR Quantitative Analysis.—We used absorbance mid-infrared spectroscopy in transmission mode as a quantitative method because it has been demonstrated (see below) that, in given conditions (described in the section on sample preparation), the amount of absorbed radiation is proportional to the quantity of absorbing matter in the sample. This means that IR absorption obeys Lambert–Beer's law. Lambert–Beer's law has been established for dilute liquid solutions, in which the analyzed component is evenly dispersed at a low concentration in a non-absorbing medium. The following relation exists when monochromatic radiation passes through an inert solution in which a substance is dissolved:

$$I = I_0 \exp(-acl)$$

where I = intensity of transmitted light, I_0 = intensity of incident light, c = concentration (mole/l), l = length of sample cell (cm), and a = absorption coefficient.

The absorbance A is defined as

$$A = \log (I_0/I) = \epsilon cl$$

where ϵ = molar extinction (or absorbance) coefficient (cm^2 $mole^{-1}$) = $(1/cl)\log(I_0/I)$

For a system in which solid particles of the substances are pressed with KBr to a transparent pellet (the KBr disc method), the following relation exists (Duyckaerts 1955, 1959):

$$A = \log(I_0/I) = \frac{m}{S\rho} \times \frac{k}{2.303}$$

where m = mass of the sample dispersed in the KBr disc, ρ = density of the particles, S = surface area of the disc normal to the beam, and k = absorption coefficient. This relation is the same as Lambert–Beer's law when $m/\rho = cl$ and $e = 2.303(k/S)$ are written.

According to Van der Marel and Beutelspacher (1976), Lambert–Beer's law is restricted to monochromatic light, non-interacting absorbers, very dilute solutions (no appreciable change in the refractive index), absence of a Christiansen effect, particle size smaller than the wavelength used, absence of scattering, linearity of the detector, and the assumption that the slits are infinitely small. Despite all these restrictions, it has been empirically demonstrated by numerous authors that mid-IR absorbance of properly ground (< 2 μm), evenly dispersed minerals at low concentration

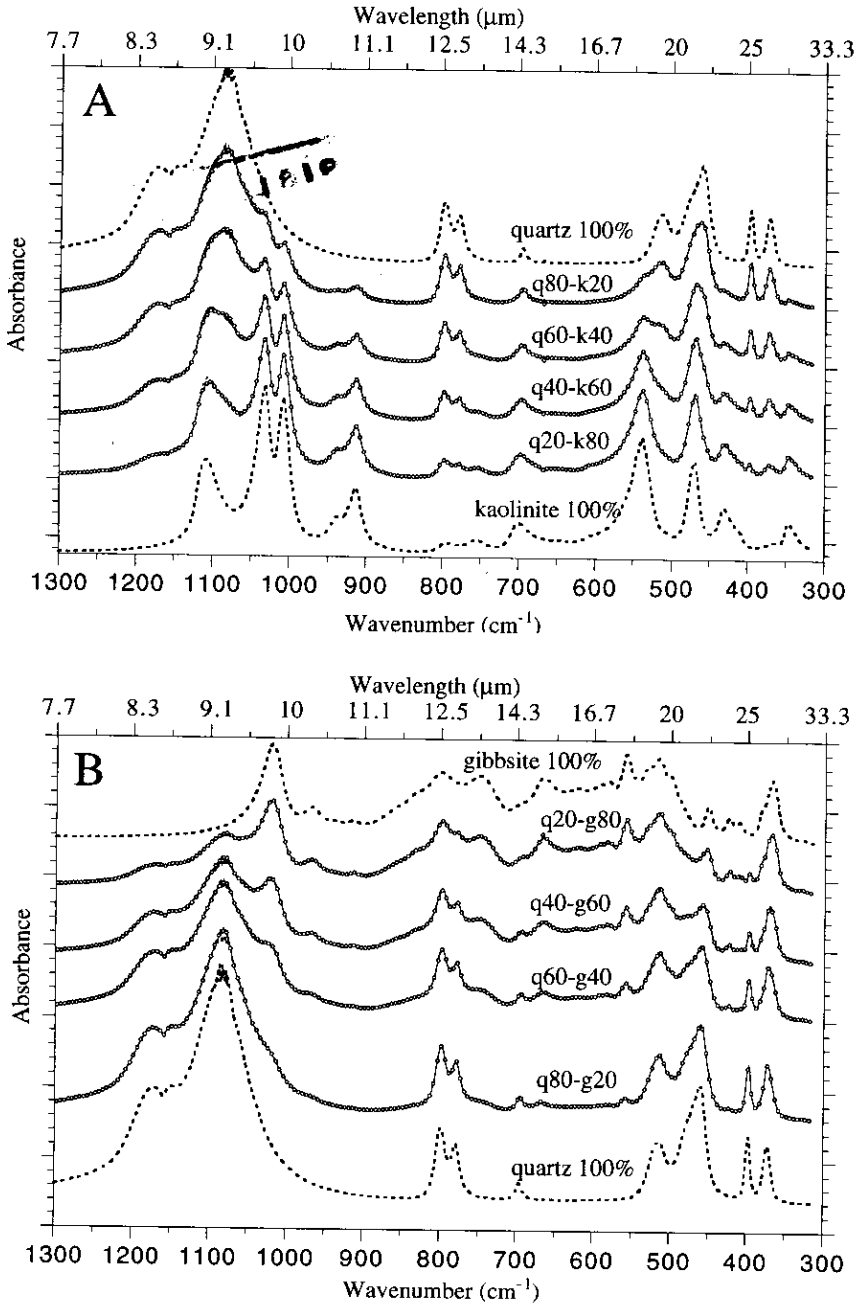

FIG. 1.—FTIR spectra of synthetic mixtures (two components). **A)** quartz–kaolinite mixtures; **B)** quartz–gibbsite mixtures; dashed curves = end member spectra; open circles = measured mixture spectra; solid curves = computed mixture spectra. q80–k20 means a mixture of 80 wt % of quartz and 20 wt % of kaolinite.

(on the order of 0.2–0.3%) in a KBr pellet shows a linear correlation with concentration; see for instance the studies of Duyckaerts (1959) for calcite, Chester and Elderfield (1967) for calcite, dolomite, and aragonite, Chester and Elderfield (1968) for amorphous silica and quartz, Van der Marel and Beutelspacher (1976) for clay minerals, Pichard and Fröhlich (1986) for quartz and calcite, and Fröhlich (1989) for silica polymorphs. This point is very important because it provides an experimental confirmation that in given conditions Lambert–Beer's law can be applied to a suspension of solid particles, as ground particles dispersed in KBr.

Sample Preparation.—All samples (reference compounds, synthetic mixtures, and natural sediments) were analyzed using KBr pellets prepared as follows: the samples were mechanically ground with small agate balls in an agate vial under acetone and in a refrigerated area (4°C) in order to prevent heating and structural changes of particles. A particle size of less than 2 μm is required to avoid excessive scattering of IR radiation. Then the powder was carefully mixed by hand with KBr in an agate mortar. A dilution of 0.25% was used for all samples studied. Weighing was performed within a dry atmosphere, with an accuracy of 10^{-5} g. A 300 mg pellet, 13 mm in diameter, was prepared by pressing the mixture in a vacuum die, with up to 8 tons·cm^{-2} of compression. The pellets were oven-dried two days at 110°C before data acquisition.

Data Acquisition.—IR spectra were recorded on a Perkin-Elmer FT 16 PC spectrometer in the 4000–250 cm^{-1} energy range with a 2 cm^{-1} resolution. For each spectrum, 50 scans were cumulated. Absorbance was computed relative to a background of sample holder containing a pure KBr pellet.

Data Reduction.—The spectral-energy range between 1315 and 315 cm^{-1} was chosen for calculation since this region yields many absorption

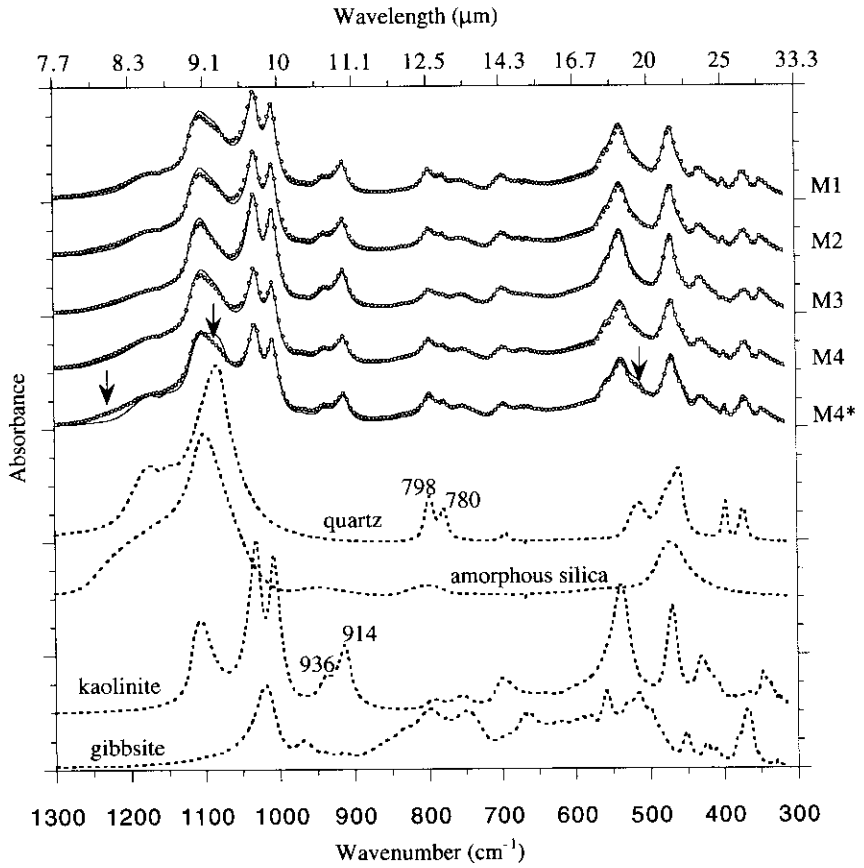

FIG. 2.—FTIR spectra of synthetic mixtures (four components). dashed curves = end-member spectra; open circles = measured mixture spectra; solid curves = computed mixture spectra; M4* indicates the superposition of the spectrum from mixture M4 and the computed spectrum using only three components (quartz + kaolinite + gibbsite); vertical arrows show region where the computed spectrum using three components differs significantly from the measured M4 spectrum, and related to the amorphous silica.

features that are relevant for distinguishing mineral components in mixture. We used the method described by Saarinen and Kauppinen (1991) for multicomponent analysis of FTIR spectra of mixtures of gases. Starting from a set of spectra of pure components, they demonstrated that the spectrum of the mixture can be mathematically processed to quantify the contribution of each component. The measured absorbance spectrum is recorded with a constant wave-vector step and thus corresponds to a $S_m(i)$ function [$i = 1, \ldots, N$], where N is the number of measured points. According to Lambert–Beer's law, the measured absorbance spectrum $S_m(i)$ of a mixture can be approximated by a computed spectrum $S_c(i)$ that is a linear combination of M reference spectra $K^j(i)$ [$j = 1,$,th. . . , M; $i = 1, \ldots, N$] recorded in the same conditions (i.e., quartz, kaolinite, . . .):

$$S_c(i) = \sum_{j=1}^{M} x_j K^j(i) \qquad [i = 1, \ldots, N]$$

Determination of the x_j coefficients to obtain a least-squares adjustment between the computed and measured spectra is done by minimizing the quantity

$$\sum_{i=1}^{N} [s'(i) - s(i)]^2$$

Calculations were performed using the "GRAPH" software (Bonnin et al. 1989). The scale factors x_j associated with each component spectrum reflect the proportion of the component in the mixture, because in our study reference spectra and mixture (artificial or natural) spectra correspond to 0.75 mg of a given constituent or blend of constituents in a 300 mg KBr pellet.

Chemical Analyses.—After drying at 60°C, the samples were crushed and sieved (200 μm). The loss on ignition (LOI) was determined by weighing after heating to 1000°C. The chemical composition was determined after melting with $LiBO_2$ and dilution in 2N HNO_3. The content of SiO_2, Al_2O_3, Fe_2O_3, TiO_2, MnO, and P_2O_5 were analyzed using ICP-AES, while Na_2O, K_2O, MgO, and CaO were analyzed using AAS. Carbon was determined with a CHN elemental analyzer.

RESULTS AND DISCUSSION

Calibration Procedure with Synthetic Mixtures

Two-Component Mixtures in KBr.—Spectra of these mixtures (quartz–kaolinite and quartz–gibbsite) were measured, and these spectra were then compared to spectra of the mineral components (Fig. 1A, B). Some characteristic spectral features can be recognized in the mixture spectra after comparison with the end-member spectra; for instance, the doublet at 914–936 cm^{-1} corresponding to the Al–OH bending vibrations of kaolinite (Van der Marel and Krohmer 1969), the doublet at 780–798 cm^{-1} due to the Si–O–Si intertetrahedral bridging bonds in quartz (Moenke 1974), and the OH deformation band of gibbsite at 1000 cm^{-1} are easily recognized. Our model was used to generate a computed mixture spectrum from the end-member spectra. The computed mixture spectra are superimposed on the measured mixture spectra (Fig. 1). The high quality of the fits shows that an IR spectrum of a two-component mixture can be calculated from the individual IR spectra of the components in the mixture. Our model was then applied to the mixture spectra in order to determine the wt % of the end members (referred to as computed wt %) in these known mixtures, which are shown in Table 1. Computed wt % of quartz, kaolinite, and gibbsite are in good agreement with the actual (weighed) wt %. The maximum relative error is 10%.

Four-Component Mixtures in KBr.—The measured spectra of the four-component mixtures (quartz, kaolinite, gibbsite, and amorphous silica)

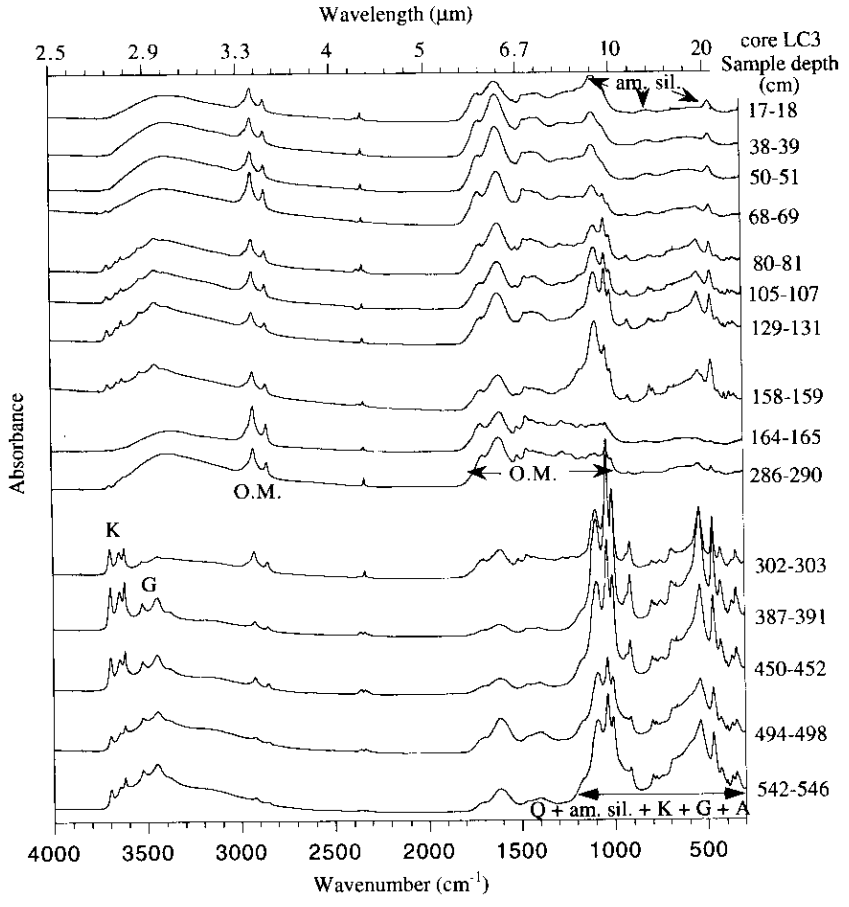

FIG. 3.—FTIR spectra from selected sediment samples from the LC3 core. O.M. = organic matter; am. sil. = amorphous silica; K = kaolinite; G = gibbsite; Q = quartz; A = anatase.

are shown in Figure 2 (open circles) together with the four end-member spectra (dashed curves). Some characteristic spectral features can be recognized in the mixture spectra after comparison with the end-member spectra; for instance, the doublet at 914–936 cm^{-1} corresponding to the Al–OH bending vibrations of kaolinite (Van der Marel and Krohmer 1969) and the doublet at 780–798 cm^{-1} due to the Si–O–Si intertetrahedral bridging bonds in quartz (Moenke 1974) are easily recognized. The computed wt % of each end member determined after application of our model are compared with the actual wt % in Table 2, and the computed mixture spectra generated from the end-member spectra by application of our model are shown (solid curves) in Figure 2. The high quality of the fit between the computed spectra (solid curves) and the measured spectra (open circles) for the four synthetic mixtures prepared is again a demonstration that our measurements obey Lambert–Beer's law. As a consequence, the spectrum of a mixture can be accurately calculated starting from the spectra of the components, as described in the section on data reduction. There is good agreement between the computed and the actual wt % for kaolinite, gibbsite, and amorphous silica (Table 2), as shown by the relative error, which is generally below 5%. For quartz, the relative error increases increasing amorphous silica content in the mixture: the relative error is 0.4%, 5%, 31%, and 30% for 5, 10, 15, and 20 wt % amorphous silica, respectively, in the mixture. The incidence of the amorphous silica content upon the accuracy of the computed quartz content is attributed to the similarity of the amorphous silica and quartz spectra: the mid-IR absorbance spectrum of amorphous silica is composed of the three fundamental vibration modes for silica, namely Si–O stretching mode at 1100 cm^{-1}, Si–O–Si stretching mode at 800 cm^{-1}, and Si–O bending mode at 470 cm^{-1} (Moenke 1974). These fundamental modes are also present in the quartz spectrum. To check this hypothesis, we applied our model to the mixture with the greater amount of amorphous silica (mixture M4, with 20% amorphous silica), using only three end-member spectra, namely quartz + kaolinite + gibbsite. We observed only slight changes in the kaolinite (43.2% instead of 42%) and gibbsite (24% instead of 25.5%) calculated wt % (Table 2). On the other hand, the calculated quartz wt % changed from 19.5% to 39.2%. The resulting computed spectrum (solid curve) differs significantly from the measured spectrum, as indicated by the arrows in Figure 2, Sample M4*. This example demonstrates that our model is sensitive to the presence of amorphous silica in a complex sample, and that it is important to check the fit between the computed and the measured spectra. Important missing end-member spectra can eventually be determined. In mixtures where quartz and amorphous silica are both present in similar proportions, the calculated quartz wt % can be significantly overestimated when the amorphous silica content is greater than 10%. This will not usually cause limitation for the mineral quantitative analysis of soils and sediments, where the quartz content is generally larger than the amorphous silica content.

Natural Sediments

Selected mid-infrared absorbance spectra of the Salitre sediments are shown in Figure 3. Several components of the sediments are easily recognized by their spectral features. Organic matter gives a set of absorption bands between 1000 and 1800 cm^{-1} (C=O, C=C, δ CH aliphatic) and a doublet between 2800 and 3000 cm^{-1} (δ CH aliphatic) (Rochdi et al. 1991; Landais et al. 1993). Bands at 3698, 3650, and 3620 cm^{-1} are due to the structural OH of kaolinite (Van der Marel and Krohmer 1969). This clay can also be recognized by the doublet at 914 and 936 cm^{-1}. The bands at 3420 and 3526 cm^{-1} indicate the presence of gibbsite (Van der Marel and Beutelspacher 1976). Small quantities of quartz are detected by the doublet

at 780 and 798 cm^{-1} (Moenke 1974). In the three samples of the top of Figure 3, the presence of amorphous silica can be recognized by the three broad bands at 470, 800, and 1100 cm^{-1} (Fröhlich 1989), because it is the only mineral phase associated with organic matter in this part of the core. Because anatase, which was identified by XRD, is always mixed with other mineral phases, no specific spectral feature can be assigned to this mineral.

Mid-IR spectral data of Figure 3, together with information from X-ray diffraction, optical microscopy, and chemical analyses (Sondag et al. 1993), show that four types of sediments are present throughout the core. At the top, between 0 and 70 cm, the sediment contains organic matter and amorphous silica represented by phytoliths. Between 70 and 160 cm, organic matter constitutes at least 80% of the sediment, but kaolinite, gibbsite, quartz, amorphous silica (phytoliths), and anatase are also present. Between 160 and approximately 300 cm, organic matter is the only constituent of the sediment. The sediment below 300 cm contains the highest proportion of kaolinite and gibbsite associated with quartz, anatase, amorphous silica, and organic matter.

Between 0 and 70 cm, the multicomponent analysis was processed using two components, organic matter + amorphous silica; the two reference spectra are shown in Figure 4A (dashed curves), together with the spectrum measured on Sample 23-24 (open circles). Below 70 cm, calculations were performed assuming that the sediments are a mixture of organic matter + quartz + kaolinite + gibbsite + anatase + amorphous silica. In Figure 4B, the reference spectra of these phases are shown (dashed curves) with spectra of two samples at 129–131 and 302–303 cm (open circles). Analysis of these natural mixtures produces wt % of various components, which are then used to generate computed spectra. The computed spectra for the various samples analyzed are shown (solid curves) superimposed upon the measured spectra (open circles) in Figure 4. The fit between the measured IR spectra of the natural sediment and the computed spectra is not as good as that observed when synthetic mixtures are processed (compare with Figures 1 and 2) but remains fairly acceptable. The resulting variations of quartz, amorphous silica, gibbsite, anatase, and kaolinite along the Salitre LC3 core are reported in Figure 5B.

Comparison with Chemical Analyses.—The three most abundant elements, except C, are Si, Al, and Ti, with the maximum values of SiO_2, Al_2O_3, and TiO_2 being 34.03%, 33.64%, and 10.39%, respectively. The high TiO_2 content of the soils and sediment (Sondag et al. 1993) is due to the particular mineralogy of the bedrock on which soils surrounding the lacustrine sediment have developed, with perovskite, calcizirtite, and apatite often present as essential minerals. Unlike TiO_2, Fe_2O_3 in sediments has a maximum value of 3.72%, and is generally lower than 3%. We have used the quantitative mineral analyses by application of our model to calculate a FTIR SiO_2, Al_2O_3, and TiO_2. The FTIR SiO_2 is the sum of the weight % of silica in quartz, amorphous silica, and kaolinite as would be stoichiometrically calculated. The FTIR Al_2O_3 is the sum of the weight % of Al_2O_3 in kaolinite and gibbsite as would be stoichiometrically calculated. The FTIR TiO_2 is equal to the weight % of anatase. Figure 5C presents the comparison between the FTIR determined and the chemically determined SiO_2, Al_2O_3, and TiO_2. One can see the very good agreement between the chemically and the FTIR determined SiO_2 (SiO_2 quartz + SiO_2 amorphous silica + SiO_2 kaolinite). For TiO_2 and Al_2O_3, the agreement is also fairly good. The slight discrepancies observed for TiO_2 can be explained by the absence of spectral features clearly related to anatase in the sediment spectra, and to minor ilmenite. For Al_2O_3 the small discrepancies could be attributed to minor phases (amorphous hydrated Al oxides possibly associated with O.M., crandallite), contamination from the aluminum coring tube, enhancing the chemical signal, and to difference of crystallinity between the natural gibbsite and the synthetic one used for calibration. In Figure 5D we determined the regression lines between chemical and FTIR SiO_2, TiO_2, and Al_2O_3; for SiO_2 and TiO_2 the regression lines that fit the data are very close to the 1/1 line. For Al_2O_3 the regression line is slightly different from the 1/1 line; compared to chemical values, Al_2O_3 FTIR values are underestimated below 8% and overestimated above 20%. The corresponding correlation coefficients (r) are 0.982, 0.954, and 0.990 for SiO_2, TiO_2, and Al_2O_3, respectively.

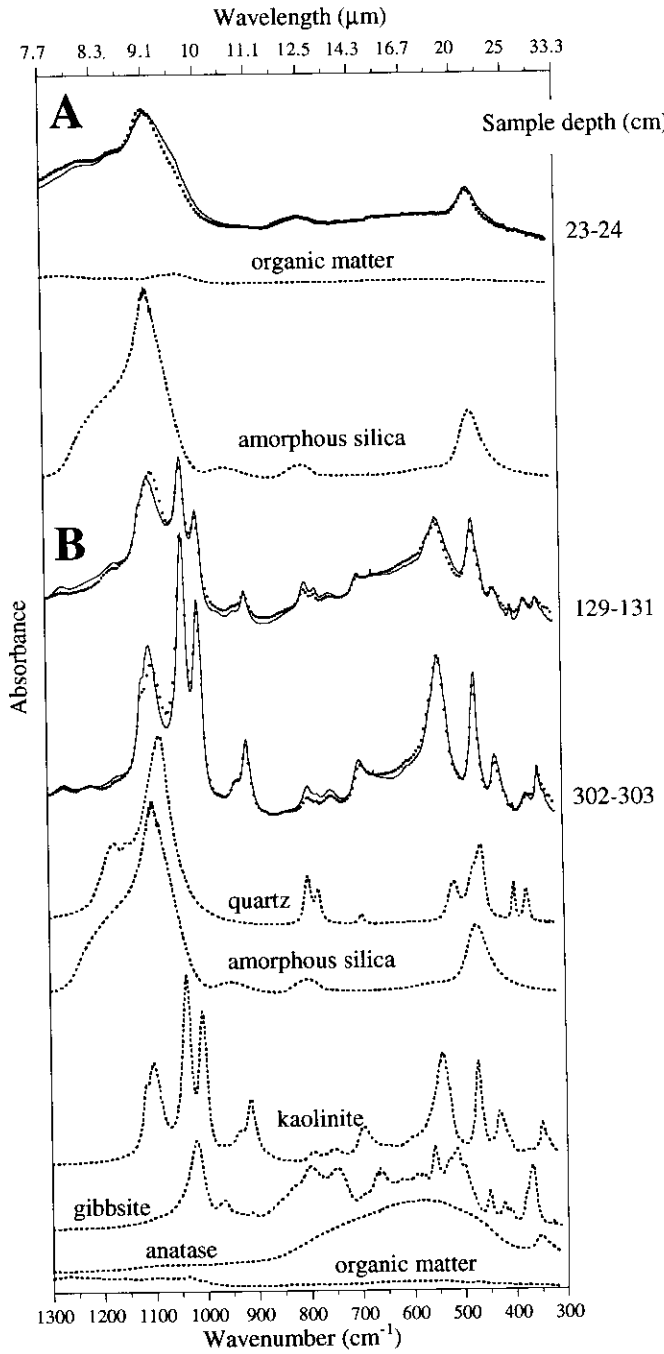

FIG. 4.—Multicomponent analysis of the Salitre sediments. **A)** spectra of the 23–24 cm sample and the two end members used to run the multicomponent analysis; **B)** spectra of the 129–131 and 302–303 samples and the six end members used to run the multicomponent analysis; dashed curves = end-member spectra; open circles = measured mixture spectra; solid curves = computed mixture spectra.

Discussion.—The rather good correlation between the FTIR and chemical SiO_2 determined on 53 samples support the quantitative results for quartz, amorphous silica, and kaolinite. The good correlation between FTIR determined wt % of anatase and TiO_2 also support the quantitative results for anatase. Although the IR spectrum of this mineral is simple, with only

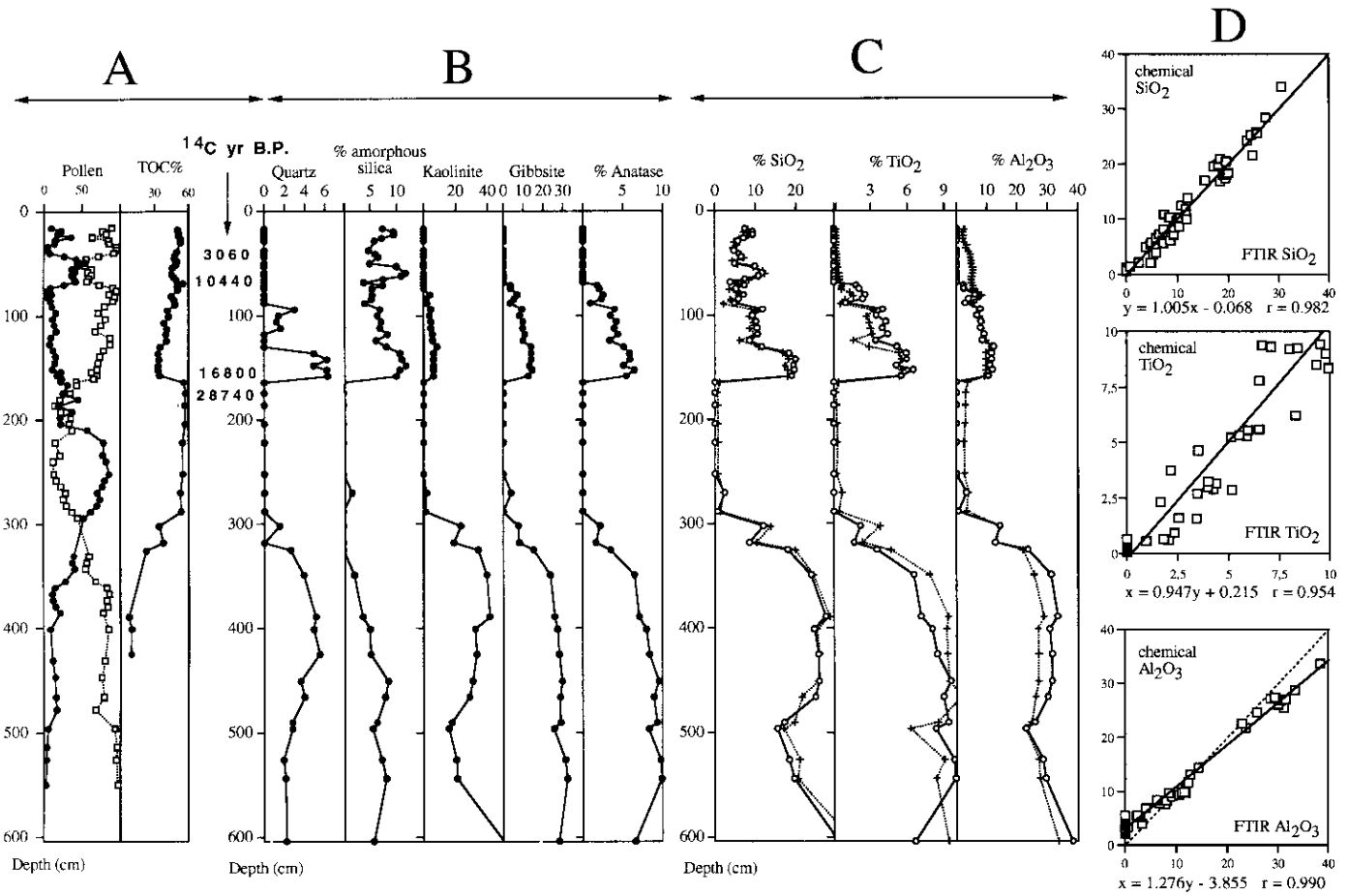

FIG. 5.—Results of the mineralogical analyses of the Salitre core; comparison with chemical, pollen and total organic carbon (TOC) data. **A)** Pollen, total organic carbon (TOC) and ^{14}C data; for the pollen column: plain circles = arboreal pollen except Myrtacea (Ledru 1996); open squares = non-arboreal pollen; **B)** Variations of mineral content along the LC3 core as determined by FTIR spectroscopy; **C)** comparison of the chemically (+) and the FTIR (o) determined (see text) SiO_2, TiO_2, and Al_2O_3. FTIR SiO_2 = SiO_2 quartz + SiO_2 amorphous silica + SiO_2 kaolinite; FTIR TiO_2 = TiO_2 anatase; FTIR Al_2O_3 = Al_2O_3 kaolinite + Al_2O_3 Gibbsite. **D)** linear regression for the chemical and FTIR determined SiO_2, TiO_2 and Al_2O_3 values. The straight lines represent the best linear fit of the data; the resulting equations and correlation coefficients (r) are given below each plot; for SiO_2 and TiO_2, the lines that fit the data are very close to the 1/1 line; for Al_2O_3, the 1/1 line is drawn as a dotted line.

two broad bands not observable when overlapped by the spectra of the other phases of our sediment, the FTIR quantitative data fit reasonably well the chemical TiO_2 determination. This confirms the results from X-ray diffraction showing that anatase is indeed the major TiO_2 phase, and shows how the multicomponent analysis of FTIR spectra can provide quantitative results on phases with no visible specific band. The quantitative determination of amorphous silica is also an advantage of FTIR spectroscopy when compared to a method like X-ray diffraction commonly used in sediment composition studies (Mumme et al. 1996).

The mineralogical similarity between the soils surrounding the depression (Sondag et al. 1993) and the sediments support the origin of kaolinite, gibbsite, quartz, and anatase from these soils. The comparison between mineralogy (Fig. 5B) and pollen contents (Ledru 1993; Ledru et al. 1996) (Fig. 5A) of the Salitre lacustrine sediments reveals an opposite trend between the forest cover, as inferred by the arboreal/non-arboreal pollen contents, and the detrital content of sediments: below 300 cm, a high content in detrital minerals corresponds to a low content in arboreal pollen; between 160 and 300 cm, an increase of the arboreal pollen/non-arboreal pollen ratio characterizes a period with a pure organic sedimentation; between 70 and 160 cm, a decrease in arboreal pollen and an increase in non-arboreal pollen coincides with the presence of detrital minerals in the sediments; above 70 cm, an increase in the arboreal pollen content matches a disappearance of the detrital phases in the sediments. This opposition between the forest development over the drainage basin and the transport of detrital phases towards the lake results from the increased susceptibility of soils to erosion after the degradation of the vegetation cover. Therefore mineral phases are tracers of regional environmental variations (Bertaux et al. 1996).

CONCLUSION

The above example demonstrates that multicomponent analysis of IR absorbance spectra is a powerful tool for quantitative mineralogical analysis of sediments. The analysis is performed on the bulk sediment after grinding. Treatments like sequential dissolution, which in many cases can affect the mineral or organic components, are not needed. Knowledge of the qualitative composition of the mixture, using X-ray diffraction analysis and microscopic observation on smear slides, is required. A second requirement is the availability of reference spectra of the various constituents. In soils or sediments, many components are susceptible to exhibiting a range of structural order/disorder and compositional variations. Clays are characterized by large variations in layer stacking and chemical compositions, both resulting in modifications of their IR absorbance spectral features, as evidenced in kaolinite minerals (Cases et al. 1982; Brindley et al. 1986) or in

smectites (Decarreau et al. 1992). In our study, we used kaolinite separated from a Brazilian soil to prepare a reference spectrum. Because only one reference spectrum per phase is required to run the calculation, this step is relatively easy to achieve provided that a good separation is made. Our study on a natural sediment shows that although we used only a limited set of reference spectra, corresponding to the main phases of the sediments, and despite the fact that the reference compounds were slightly different from the natural one, we obtained FTIR determined wt % of the mineral phases consistent with available chemical data. This suggests that our method can be applied to a large variety of natural mixtures. The multicomponent analysis of IR absorbance spectra succeeds in quantifying components identified by XRD (anatase) or optical microscopy (amorphous silica) but with no visible spectral features in the mixture spectrum. This is a great advantage over previous use of IR absorbance spectroscopic data for quantifying mineral phases by measuring specific band surface (Fröhlich 1982; Sifeddine et al. 1994; Chester and Elderfield 1968; Fröhlich and Servant-Vildary 1989). Correlation between pollen data and quantitative mineralogy in the Salitre sediments reveals that degradation of the vegetal cover is the main factor that controls the transport of the detrital minerals (quartz, kaolinite, gibbsite, and anatase) from the surrounding soils towards the lake. Because changes in the vegetal cover result from climatic variability, the mineral content of the lacustrine sediments can be used as an indicator of environmental changes.

ACKNOWLEDGMENTS

This work was supported by the UR 12 of the "Terre-Océan-Atmosphère" Department of Institut Français de Recherche Scientifique pour le Développement en Coopération (ORSTOM). It is part of the AIMPACT–PVC (ORSTOM) and "ECOFIT" (CNRS–ORSTOM) programs. Caroline Duong is greatly acknowledged for her contribution in the samples preparation and analysis. The authors wish to thank F. Sondag, L. Martin, J.M. Flexor, G. Morin, and T. Corrège for their help during the preparation of the manuscript. J.L. Bishop and an anonymous reviewer are thanked for their critical reading of the manuscript and helpful suggestions.

REFERENCES

Balsam, W.L., and Deaton, B.C., 1996, Determining the composition of late Quaternary marine sediments from NUV, VIS and NIR diffuse reflectance spectra: Marine Geology, v. 134, p. 31–55.

Barranco, F.T., Balsam, W.L., and Deaton, B.C., 1989, Quantitative reassessment of brick red lutites: evidence from reflectance spectrophotometry: Marine Geology, v. 89, p. 299–314.

Bertaux, J., Ledru, M.P., Soubiès, F., and Sondag, F., 1996, The use of quantitative mineralogy linked to palynological studies in palaeoenvironmental reconstruction: the case study of the "Lagoa Campestre" lake, Salitre, Minas Gerais, Brazil: Académie des Sciences [Paris], Comptes Rendus, v. 323, série II a, p. 65–71.

Bishop, J.L., Koeberl, C., Kralik, C., Fröschl, H., Englert, P.A.J., Andersen, D.W., Pieters, C.M., and Wharton, R.A., Jr., 1996, Reflectance spectroscopy and geochemical analyses of Lake Hoare sediments, Antarctica: Implications for remote sensing of the Earth and Mars: Geochimica et Cosmochimica Acta, v. 60, p. 765–785.

Bonnin, D., Kaiser, P., Fretigny, C., and Debarbies, J., 1989, Logiciel d'analyse sur microordinateur IBM-PC, *in* Dexpert, H., Michałowicz, A., and Verdaguer, M., eds, Structures fines d'absorption des rayons X en chimie, Ecole du CNRS, Orsay-Garchy, 19–24 Septembre 1988, Orsay, v. 3-2, p. 1–32.

Brindley, G.W., Kao, C.C., Harrison, J.L., Lipsicas, M., and Raythatha, R., 1986, Relation between structural disorder and other characteristics of kaolinites and dickites: Clays and Clay Minerals, v. 34, p. 239–249.

Cases, J.M., Liétard, O., Yvon, J., and Delon, J.F., 1982, Etude des propriétés cristallochimiques, morphologiques et superficielles de kaolinites désordonnées: Bulletin de Minéralogie, v. 105, p. 439–457.

Chester, R., and Elderfield, H., 1967, The application of infra-red absorption spectroscopy to carbonate mineralogy: Sedimentology, v. 9, p. 5–21.

Chester, R., and Elderfield, H., 1968, The infrared determination of opal in siliceous deep-sea sediments: Geochimica et Cosmochimica Acta, v. 32, p. 1128–1140.

Dean, W.E., 1993, Physical properties, mineralogy, and geochemistry of Holocene varved sediments from Elk lake, Minnesota, *in* Bradbury, J.P., and Dean, W.E., eds., Elk Lake, Minnesota: Evidence for Rapid Climate Change in the North-Central United States: Geological Society of America, Special Paper 276, p. 135–157.

Deaton, B.C., and Balsam, W.L., 1991, Visible spectroscopy—A rapid method for determining hematite and goethite concentration in geological materials: Journal of Sedimentary Petrology, v. 61, p. 628–632.

Decarreau, A., Grauby, O., and Petit, S., 1992, The actual distribution of octahedral cations in 2:1 minerals: Results from clay synthesis: Applied Clay Science, v. 7, p. 147–167.

Drees, L.R., Manu, A., and Wilding, L.P., 1993, Characteristics of aeolian dusts in Niger, West Africa: Geoderma, v. 59, p. 213–233.

Duyckaerts, G., 1955, Contribution à l'analyse quantitative par les spectres d'absorption infrarouge des poudres. I. Examen théorique de la question: Spectrochimica Acta, v. 7, p. 25–31.

Duyckaerts, G., 1959, The infrared analysis of solid substances: Analyst, v. 84, p. 201–214.

Farmer, V.C., ed., 1974, The infrared spectra of minerals: Mineralogical Society [London], Monograph 4, 539 p.

Fretigny, C., and Desbarres, J., 1988, Graph: software for "Ecole CNRS: structures fines d'absorption des rayons X. Des données expérimentales à leur analyse".

Fröhlich, F., 1982, Evolution minéralogique dans les dépots azoïques rouges de l'océan indien. Relations avec la stratigraphie: Société Géologique de France, Bulletin, v. 3, p. 563–571.

Fröhlich, F., 1989, Deep-sea biogenic silica: new structural and analytical data from infrared analysis—geological implications: Terra Nova, v. 1, p. 267–273.

Fröhlich, F., and Servant-Vildary, S., 1989, Evaluation of diatom content by counting and infrared analysis in quaternary fluvio-lacustrine deposits from Bolivia: Diatom Research, v. 4, p. 241–248.

Gaffey, S.J., McFadden, L.A., Nash, R., and Pieters, C., 1993, Ultraviolet, visible, and near-infrared reflectance spectroscopy: Laboratory spectra of geologic materials, *in* Pieters, C.M., and Englert, P.A.J., eds., Remote Geochemical Analysis: Elemental and Mineralogical Composition, Cambridge University Press, p. 43–77.

Gehlen, M., and Van Raaphorst, W., 1993, Early diagenesis of silica in sandy North Sea sediments: quantification of the solid phase: Marine Chemistry, v. 42, p. 71–83.

Jones, J.B., and Segnit, E.R., 1971, The nature of opal I. Nomenclature and constituent phases: Geological Society of Australia, Journal, v. 18, p. 57–68.

Jones, R.L., 1969, Determination of opal in soil by alkali dissolution analysis: Soil Science Society of America, Proceedings, v. 33, p. 976–978.

Landais, P., Rochdi, A., Largeau, C., and Derenne, S., 1993, Chemical characterization of torbanites by transmission micro-FTIR spectroscopy: origin and extent of compositional heterogeneities: Geochimica et Cosmochimica Acta, v. 57, p. 2529–2539.

Ledru, M.P., 1993, Late Quaternary Environmental and climatic changes in central Brazil: Quaternary Research, v. 39, p. 90–98.

Ledru, M.P., Soares Braga, P.I., Soubiès, F., Fournier, M., Martin, L., Suguio, K., and Turcq, B., 1996, The last 50,000 years in the Neotropics (Southern Brazil): evolution of vegetation and climate: Palaeogeography, Palaeoclimatology, Palaeoecology, v. 123, p. 239–257.

Moenke, H.H.W., 1974, Silica, the three dimensional silicates, borosilicates and beryllium silicates, *in* Farmer, V.C., ed., The Infrared Spectra of Minerals: Mineralogical Society [London], Monograph 4, p. 365–382.

Mumme, W.G., Tsambourakis, G., Madsen, I.C., and Hill, R.J., 1996, Improved petrological modal analyses from X-ray powder diffraction data by use of the Rietveld method, Part II. Selected sedimentary rocks: Journal of Sedimentary Research, v. 66, p. 132–138.

Mustard, J.F., and Pieters, C.M., 1989, Photometric phase functions of common geologic minerals and applications to quantitative analysis of mineral mixture reflectance spectra: Journal of Geophysical Research, v. 94, p. 13,619–13,634.

Pichard, C., and Fröhlich, F., 1986, Analyses IR quantitatives des sédiments. Exemple du dosage du quartz et de la calcite: Institut Français du Pétrole, Revue, v. 41, p. 809–819.

Rochdi, A., Landais, P., and Burneau, A., 1991, Analysis of coal by transmission FTIR microspectroscopy: methodological aspect: Société Géologique de France, Bulletin, v. 162, p. 155–162.

Rognon, P., Coude-Gaussen, G., Revel, M., Grousset, F.E., and Pedemay, P., 1996, Holocene Saharan dust deposition on the Cape Verde Islands: sedimentological and Nd–Sr isotopic evidence: Sedimentology, v. 43, p. 359–366.

Saarinen, P., and Kauppinen, J., 1991, Multicomponent analysis of FT–IR spectra: Applied Spectroscopy, v. 45, p. 953–963.

Salisbury, J.W., 1993, Mid-infrared spectroscopy: Laboratory data, *in* Pieters, C.M., and Englert, P.A.J., eds., Remote Geochemical Analysis: Elemental and Mineralogical Composition, Cambridge University Press, p. 79–98.

Sifeddine, A., Fröhlich, F., Fournier, M., Martin, L., Servant, M., Soubiès, F., Turcq, B., Suguio, K., and Volkmer-Ribeiro, C., 1994, La sédimentation lacustre indicateur de changement des paléoenvironnements au cours des 30 000 dernières années (Carajas, Amazonie, Brésil): Académie des Sciences [Paris], Comptes Rendus, v. 318, p. 1645–1652

Sondag, F., Soubiès, F., Fortune, J.P., Dupré, B., Magat, P., and Melfi, A., 1996, Hydrogeochemistry in soils and sediments in the area of the Lagoa Campestre lake (Salitre, MG, Brazil): chemical balances of major and trace elements and dynamics of rare earth elements: Applied Geochemistry, v. 12, p. 155–162.

Sondag, F., Soubiès, F., Ledru, M.P., and Delacne, M., 1993, Geochemical markers of palaeoenvironments: relations between climatic changes, vegetation and geochemistry of lake sediments, southern Brazil: Applied Geochemistry, Supplementary Issue no. 2, p. 165–170.

Sunshine, J.M., and Pieters, C.M., 1993, Estimating modal abundances from the spectra of natural and laboratory pyroxene mixtures using the modified gaussian model: Journal of Geophysical Research, v. 98, p. 9075–9087.

Tessier, A., Campbell, P.G.C., and Bisson, M., 1979, Sequential extraction procedure for the speciation of particulate trace metals: Analytical Chemistry, v. 51, p. 844–851.

Van der Marel, H.W., and Krohmer, P., 1969, OH stretching vibrations in kaolinite, and related minerals: Contributions to Mineralogy and Petrology, v. 22, p. 73–82.

Van der Marel, H.W., and Beutelspacher, H., 1976, Atlas of infrared spectroscopy of clay minerals and their admixtures: Amsterdam, Elsevier, 396 p.

Received 27 September 1996; accepted 9 December 1997.